Micromechanical Models for the Brownian Motion of Hair Cell Stereocilia

Wolfgang A. Svrcek-Seiler*, Ilse C. Gebeshuber*, Frank Rattay‡,
Tamás S. Biro† and Harald Markum*

*TU-BioMed, Vienna University of Technology, Wiedner Hauptstr 8–10, A-1040 Vienna,
Austria and †MTA RMKI, Research Institute for Particle and Nuclear Physics, H-1525
Budapest, Hungary*

Brownian motion of the hairs (stereocilia) of amphibian hair cells has been shown in experiments to be in the range of some nm. Our models of the Brownian motion of coupled harmonic oscillators with mechanical properties of stereocilia lead to similar displacements. Computer simulation shows that stochastic fluctuations enhance the encoding of low level acoustic signals. Stochastic resonance lowers the detection threshold of auditory signals to amplitudes one order of magnitude lower than that of the Brownian motion.

© 1998 Academic Press

Introduction

The stochastic contribution by thermal motion to movements of the elastic structures in the inner ear essentially depends on their masses: at the basilar membrane, the thermal influence is negligible, at the tiny hairs (stereocilia) of the receptor cells it is relatively large, i.e. in the range of 2 nm. At the threshold of hearing, acoustic stimuli cause vibrations of the stereocilia in the order of some hundreds of picometers (Hudspeth, 1989), this means that at the receptor cell the influence of thermal noise is 10 times higher than that of the acoustic signal.

The fact that thermal motion is not audible was the basis for controversies about the actual vibration amplitudes at the threshold of hearing (e.g. de Vries, 1948). Harris (1967) proposed the hypothesis that the stereocilia of every auditory receptor cell have to be strongly coupled to reduce the amplitude of their Brownian motion. Years later, electron microscopy revealed two types of connections between the stereocilia: tip links and lateral links, which act as springs and keep the hairs together (Flock *et al.*, 1977; Pickles *et al.*, 1984).

Spontaneous activity in single nerve fibers was measured to be up to 140 spikes/s and is present in the absence of any acoustic stimulation (Relkin & Doucet, 1991). Note that this spontaneous spiking does not lead to any sensory perception which reflects the ability of the brain to suppress noise. In this article we show that Brownian motion contributes to the spontaneous activities of auditory nerve fibers.

Hair cells in sensory systems detect fluid motions, in the lateral line organ in fish as well as in the vestibular and in the hearing organ. The stereocilia of a typical mammalian auditory inner hair cell are arranged in three rows of increasing height, with 20 stereocilia in each row (for physiological details see Fig. 1). There is a variability in the number and the arrangement of stereocilia per hair cell, e.g. in the apex of the guinea pig cochlea some outer hair cells have less than three rows of stereocilia.

Mechanical Model of Stereocilia Motion

A single stereocilium is modeled as a stiff rod with two degrees of freedom, which is ball jointed to the

‡Author to whom correspondence should be addressed at:
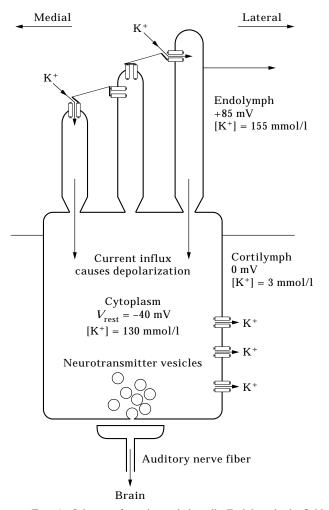Vienna University of Technology, Wiedner Hauptstr., 8-10/114, A-1040, Austria.

FIG. 1. Scheme of an inner hair cell. Endolymphatic fluid motions caused by the movement of the hearing ossicles induce displacements of the hairs (stereocilia) of the auditory receptor cell. The stereocilia of one inner hair cell are interconnected by links (elastic protein filaments). The open–close kinetics of the transduction channels located close to the top of each stereocilium depend on stereociliary deflection. Even in the resting state the transduction channel open probability is about 15%. Due to potential gradients, ion currents (mainly potassium) enter the cell through the transduction channels and leave through ion channels in the cell body membrane, causing a resting potential of about -40 mV in the unstimulated hair cell and potential changes of some mV following stereociliary displacements. A potential change as low as 0.1 mV may cause neurotransmitter release and thereby a spike in one of the connecting auditory nerve fibers. Note the tapering of the stereocilia bottom endings. In humans the inner hair cell stereocilia are arranged in a 20×3 matrix with 20 short, 20 middle and 20 long elements; each stereocilium behaves like a rigid rod pivoting around its insertion to the cuticular plate.

cuticular plate at the apical end of the cell body. Therefore the moment of inertia is $I = ml^2/3$, where m and l denote stereocilia mass and length. The movement of the tips of the stereocilia can be regarded as a two-dimensional problem, since in the normal range of operation the displacements are about 0.01 of stereocilia length, and result from

solving the following uncoupled Langevin equations of motion:

$$\ddot{x} + \beta\dot{x} + \omega_0^2 x = X(t), \quad \ddot{y} + \beta\dot{y} + \omega_0^2 y = Y(t) \quad (1)$$

where x and y are the displacements of the stereocilia tips, β is the damping constant, ω_0 in eqn (1) denotes the undamped angular eigenfrequency. Note that $\omega_0 = \sqrt{3C/m}$, where C, the stiffness of a stereocilium, is measured as the ratio between an external horizontal force applied to the tip of the stereocilium and the resulting horizontal tip displacement. $X(t)$ and $Y(t)$ are the accelerations due to the stochastic driving forces (thermal motions of the cochlear fluids) and correspond to a white noise. It is characterized by the spectral density $2kT/m\cdot\beta$ with the Boltzmann constant k, the absolute temperature T and the mass m of the stereocilium. For computational reasons we modeled the effect of the white noise as a random acceleration which is constant during one integration step Δt. The standard deviation of the random acceleration is

$$\sqrt{\frac{2kT}{m\cdot\Delta t}\cdot\beta}.$$

THREE ELASTICALLY COUPLED STEREOCILIA WITH INCREASING LENGTHS

We consider the Brownian motion of a subsystem of the hair bundle of an inner hair cell (IHC) in the physiologically relevant x-coordinate. Only displacements along the x-axis influence the open–close kinetics of the mechano-sensitive transduction channels: displacement to the lateral side increases their open probability, displacement to the medial side results in a decrease of the open probability. According to the mechanical scheme shown in Fig. 2, this subsystem consists of three elastically coupled stereocilia with increasing lengths. The resulting coupled Langevin equations of motion are:

$$\ddot{x}_1 + \beta_1\dot{x}_1 + \omega_{0,1}^2 x_1 - \frac{3Kl_2}{m_1 l_1}\left(x_2 - \frac{l_2}{l_1}x_1 + l_0\right) = X_1(t)$$

(2a)

$$\ddot{x}_2 + \beta_2\dot{x}_2 + \omega_{0,2}^2 x_2 + \frac{3K}{m_2}\left(x_2 - \frac{l_2}{l_1} + l_0\right)$$

$$- \frac{3Kl_3}{m_2 l_2}\left(x_3 - \frac{l_3}{l_2}x_2 + l_0\right) = X_2(t) \quad (2b)$$

$$\ddot{x}_3 + \beta_3\dot{x}_3 + \omega_{0,3}^2 x_3 + \frac{3K}{m_3}\left(x_3 - \frac{l_3}{l_2}x_2 + l_0\right) = X_3(t)$$
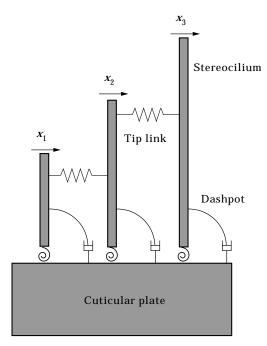
(2c)

FIG. 2. Equivalent mechanical system of three stereocilia of increasing height. The tip links, connections between the rigid rods representing the stereocilia, are modeled as springs.

where K denotes the stiffness of the coupling springs, l_0 the tip link length without tension and l_1, l_2, l_3 are the stereocilia lengths.

For the parameters given in Table 1, the root-mean-square displacements of the short (1 μm), the middle (1.6 μm) and the long (4 μm) stereocilia are 1.4, 1.8 and 4.2 nm, respectively. A 1 ms portion of the time evolution of the displacements and corresponding spectral densities are presented in Fig. 3. The amplitude of the spectral density (right traces in Fig. 3) is proportional to the square of the stereocilia length. Note the decrease of the spectral densities for the displacements of the long and middle stereocilia at higher frequencies (Fig. 3). The high frequency contributions are most relevant for the movement of the short stereocilia. Denk *et al.* (1989) report spectral densities of similar shape for the displacements due to Brownian motion of the stereocilia bundle of amphibian hair cells. The influence of the two shorter stereocilia on the Brownian motion of the long stereocilium is in spite of the very small stiffness and pre-tension of the elastic coupling in the range of a few per cent.

THE LINEAR CHAIN AS A MODEL FOR THE STEREOCILIARY BUNDLE

There are several connections of a single stereocilium to its neighbors and the forces exerted by those lateral and tip links operate at different height. A detailed three-dimensional model would represent each of them as a spring. A simplified version of the complex situation is shown in Fig. 4. This system can be simplified by incorporating the effects of the second and third rows of stereocilia by introducing transversal forces between the adjacent masses in the first row stereocilia. The reduced system is shown by the solid lines in Fig. 4. Therefore the Brownian motion of the complete human IHC hair bundle can be modeled with reduced effort: instead of 60 stereocilia in three rows, a linear chain of 20 elastically coupled (averaged stiffness K) two-dimensional harmonic oscillators with increased stiffness C to compensate for the neglected elements is used.

Each of these harmonic oscillators represents three elastically coupled stereocilia with increasing lengths: the influence of the two rows of shorter stereocilia is included as a strengthened elastic coupling of the single oscillator to its resting state.

TABLE 1

Parameters used for modeling the three elastically coupled stereocilia with increasing lengths

Damping constants of the long, the middle and the short stereocilia (Bialek & Schweitzer, 1987)	$\beta_1 = 6.0 \cdot 10^6$ s^{-1}
	$\beta_2 = 2.4 \cdot 10^6$ s^{-1}
	$\beta_3 = 1.5 \cdot 10^6$ s^{-1}
Length of tip link without tension (guinea pig, Zetes, 1995)	$l_0 = 20$ nm
Lengths of the long, the middle and the short stereocilia (guinea pig, Zetes, 1995)	$l_1 = 4.0$ μm
	$l_2 = 1.6$ μm
	$l_3 = 1.0$ μm
Masses of the long, the middle and the short stereocilia (Bialek & Schweitzer, 1987; guinea pig, Zetes, 1995)	$m_1 = 2.2 \cdot 10^{-16}$ kg
	$m_2 = 8.0 \cdot 10^{-17}$ kg
	$m_3 = 5.0 \cdot 10^{-17}$ kg
Stiffness of the tip links (guinea pig, Zetes, 1995)	$K = 5.0 \cdot 10^{-4}$ Nm^{-1}
Undamped angular eigenfrequencies of the long, the middle and the short stereocilia (Bialek & Schweitzer, 1987; guinea pig, Steele & Jen, 1988)	$\omega_{0,1}^2 = 8.3 \cdot 10^{11}$ s^{-2}
	$\omega_{0,2}^2 = 4.9 \cdot 10^{12}$ s^{-2}
	$\omega_{0,3}^2 = 1.3 \cdot 10^{13}$ s^{-2}

FIG. 3. Simulated time series (left) and spectral densities (right) of the displacements of the long, medium and short stereocilia (top, middle and bottom traces, respectively). Spectral densities were obtained from 16 000 data points; the arrow indicates the knee frequency. The spectral density of the long stereocilium is fitted with a Lorentzian

$$\frac{2A\overline{\omega}}{\pi \cdot (\overline{\omega}^2 + 4(f - f_c)^2)} \quad \text{with} \quad A = 23.3 \text{ Hz}, \ \overline{\omega} = 18\,700 \text{ Hz}, \ f_c = 3907 \text{ Hz}.$$

The Langevin equations of motion for the inner elements of the chain are

$$\ddot{x}_i + \beta_i \dot{x}_i + \omega_0^2 x_i - (a_{x,i} - a_{x,i-1}) = X_i(t),$$

$$\ddot{y}_i + \beta_i \dot{y}_i + \omega_0^2 y_i - (a_{y,j} - a_{y,i-1}) = Y_i(t) \qquad (3a)$$

with $i = 2, \ldots, 19$.

The Langevin equations of motion for the top and bottom ends of the chain are

$$\ddot{x}_1 + \beta_1 \dot{x}_1 + \omega_0^2 x_1 - a_{x,1} = X_1(t),$$

$$\ddot{y}_1 + \beta_1 \dot{y}_1 + \omega_0^2 y_1 - a_{y,1} = Y_1(t) \qquad (3b)$$

$$\ddot{x}_{20} + \beta_{20} \dot{x}_{20} + \omega_0^2 x_{20} + a_{x,19} = X_{20}(t),$$

$$\ddot{y}_{20} + \beta_{20} \dot{y}_{20} + \omega_0^2 y_{20} + a_{y,19} = Y_{20}(t). \qquad (3c)$$
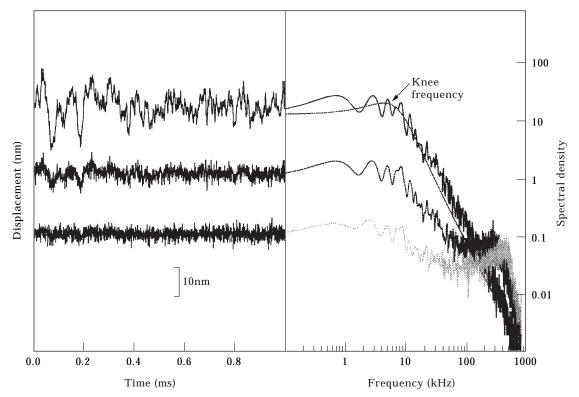
The accelerations due to the elastic coupling are

$$a_{x,i} = \Omega_0^2 \left(\sqrt{(x_{i+1} - x_i)^2 + (y_{i+1} - y_i + d_0)^2} - \lambda d_0 \right)$$

$$\times \frac{x_{i+1} - x_i}{\sqrt{(x_{i+1} - x_i)^2 + (y_{i+1} - y_i + d_0)^2}} \qquad (4)$$

and

$$a_{y,i} = \Omega_0^2 \left(\sqrt{(x_{i+1} - x_i)^2 + (y_{i+1} - y_i + d_0)^2} - \lambda d_0 \right)$$

$$\times \frac{y_{i+1} - y_i + d_0}{\sqrt{(x_{i+1} - x_i)^2 + (y_{i+1} - y_i + d_0)^2}} \qquad (5)$$

with $\Omega_0^2 = 3K/m$ and d_0 the initial distance between the masses (50 nm). The parameter that regulates the pre-tension of the coupling springs between two adjacent masses is λ ($0 < \lambda < 1$), without pre-tension $\lambda = 1$. For additional transversal elastic coupling attractive forces appear in the x-direction, which are in the presented model proportional to the difference of the x-coordinates of neighboring masses: in this case, the term $a_{x,i}^{Tr} = \Omega_{Tr}^2 (x_{i+1} - x_i)$ has to be added to the acceleration $a_{x,i}$ (see Fig. 4). The values of the parameters used for modeling are given in Table 2.

In the following we present three case studies in order to show some synchronizing effects of the displacements of the single elements of the chain, caused by the pre-tension of the coupling springs which connect the masses in the y-direction. In the simplest case the masses are connected via springs
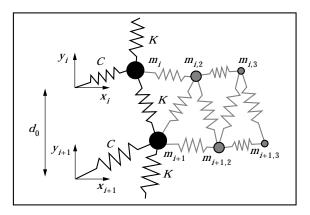
FIG. 4. Top view of the linear chain as a model of the stereociliary bundle (simplified). The solid lines represent the reduced system, the gray elements complete the 3×20 structure of the hair bundle. The resting states of the masses m_i are in the origins of the respective coordinate systems, the initial distance between the masses is d_0. C denotes the stiffness and K the spring constant of longitudinal coupling.

elements 11–20 is smaller than the estimated error [Fig. 5(b)]. The linear chain of oscillators is a simplified model of the stereociliary bundle which consists of three parallelly coupled chains. The real structure of the coupling elements within the stereociliary bundle is not yet completely known, the effect of possible inner coupling is modeled in case 3 as additional longitudinal stiffness (transversal elastic coupling of the oscillators: $a_{x,i}^{Tr} = \Omega_{Tr}^2 (x_{i+1} - x_i)$, with $\Omega_{Tr}^2 = 70\Omega_0^2$). Because of the additional coupling the mean displacement is smaller than in the two previous cases and the correlation is larger. Note that in this case the transversal coupling was chosen to be about eight times stronger than the longitudinal one, to clearly illustrate the effects.

The Mechano-electrical Transduction at the Threshold of Hearing

A reduced model for the mechano-electrical transduction in inner hair cells (Rattay *et al.*, 1998a) is used to show the amplifying influence of the Brownian motion on the threshold of the detection of auditory signals. The potential fluctuations within the hair cell are modeled using equivalent electric circuits for cell membrane and cytoplasm (RC-components and batteries), the kinetics of the transduction channels are modeled as Markov processes with a linear relation between the stereociliary displacement and the open probability in the region of displacements of a few mn. The inner hair cell membrane time constant is $\tau = 0.255$ ms, therefore the inner hair cell potential is a low-pass filtered picture of the stereociliary displacements with additional noise because of the stochastic components in channel gating (Fig. 6).

In sensitive release zones of the hair cells a potential change exceeding 0.1 mV above the resting potential is enough to trigger neurotransmitter release and thus

without pre-tension ($\lambda = 1$). According to Hook's law, the back-driving forces are proportional to the displacement. The mean transversal displacements of the coupled oscillators are nearly constant along the chain, since the elastic potential is mainly determined by the coupling of each oscillator to the resting state [Fig. 5(a), upper trace], and close to the displacements of single oscillators without any longitudinal coupling (data not shown). The correlation of the Brownian motion within the chain is below statistical fluctuations. In the case with pre-tension ($\lambda = 0.2$), the longitudinally coupled springs cause a linear transversal coupling, i.e. a spring force which is proportional to the transversal component of the distance to neighboring oscillators. The correlation of the movements is stronger compared with the $\lambda = 1$ case and theoretically does not vanish along the whole chain. Because of the finite number of elements in the ensemble the correlation of the first element to the

TABLE 2

Parameters used for the linear chain as a model for the stereociliary bundle

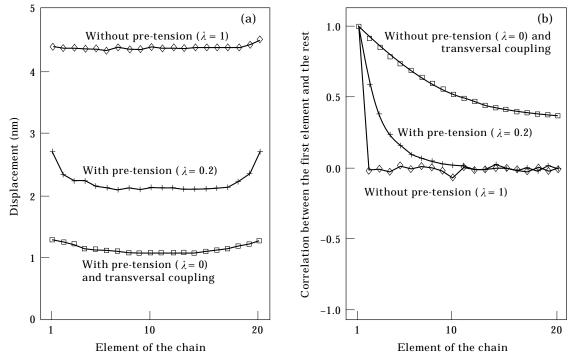|	
Damping constant (Bialek & Schweitzer, 1987)	$\beta = 6.0 \cdot 10^6$ s^{-1}
Initial distance between the masses (guinea pig, Zetes, 1995)	$d_0 = 50$ nm
Length of stereocilium (guinea pig, Zetes, 1995)	$l = 4.0$ µm
Longitudinal coupling constant (Bialek & Schweitzer, 1987; guinea pig, Zetes, 1995)	$\Omega_0^2 = 2.0 \cdot 10^{12}$ s^{-2}
Mass (Bialek & Schweitzer, 1987; guinea pig, Zetes, 1995)	$m = 2.2 \cdot 10^{-16}$ kg
Parameter regulating the pre-tension of the coupling springs	$0 < \lambda \leqslant 1$
Spring constant of longitudinal coupling (guinea pig, Zetes, 1995)	$K = 5.0 \cdot 10^{-4}$ Nm^{-1}
Stiffness (guinea pig, Zetes, 1995)	$C = 2.2 \cdot 10^{-4}$ Nm^{-1}
Transversal elastic coupling constant (Bialek & Schweitzer, 1987; guinea pig, Zetes, 1995)	$\Omega_{Tr}^2 = 1.4 \cdot 10^{14}$ s^{-2}
Undamped angular eigenfrequency (Bialek & Schweitzer, 1987; guinea pig, Steele & Jen, 1988); effective angular frequency	$\omega_0^2 = 8.3 \cdot 10^{11}$ s^{-2} $\omega_0^2 = 9.9 \cdot 10^{11}$ s^{-2}

FIG. 5. Influence of pre-tension and transversal coupling on the 20 elements of the linear chain model: (a) r.m.s. displacement; (b) correlation of the displacement of the first oscillator with that of the other elements of the chain.

an action potential can be generated in the auditory nerve (Hudspeth, 1989). Figure 7 demonstrates that the voltage fluctuations due to a weak signal alone would rarely reach threshold, however additional fluctuations caused by Brownian motion help to generate spikes. The spiking rate caused by a very weak signal does not exceed the spontaneous rate but

the nerve impulses become, with increasing signal strength, more and more phase-locked to the maxima of the acoustic input, i.e. with increasing signal-to-noise ratio the spiking pattern becomes more regular.
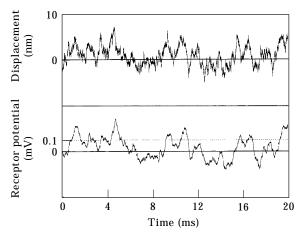

FIG. 6. Mechanical and electrical fluctuations due to Brownian motion: the intracellular receptor potential changes are a low-pass filtered picture of stereociliary displacements with an additional portion of noise resulting from the transduction channel kinetics. The time constant ($\tau = 0.255$ ms) is calculated from the exponential voltage time course following a stimulus that immediately opens all of the transduction channels (Rattay et al., 1998a).
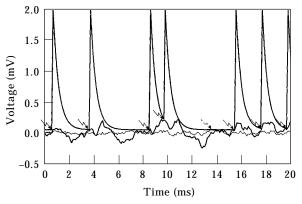

FIG. 7. Simulation receptor potential changes and resulting firing behavior. The voltage evoked by the weak sinusoidal signal alone (thin line, hypothetical case without Brownian motion) is fluctuating because of transduction channel kinetics. Only in one case (marked by dashed arrow at 13.5 ms) those fluctuations are large enough to reach the threshold of spiking at 0.1 mV. The compound fluctuations caused by sinusoidal tone plus noise with a signal-to-noise ratio of 1/10 produce seven spikes within 20 ms that are distributed to connecting auditory nerve fibers. The recovery behavior after spiking is modeled by an exponential decay of the threshold curve: as soon as the voltage fluctuations cross the threshold curve again, a new spike can occur.
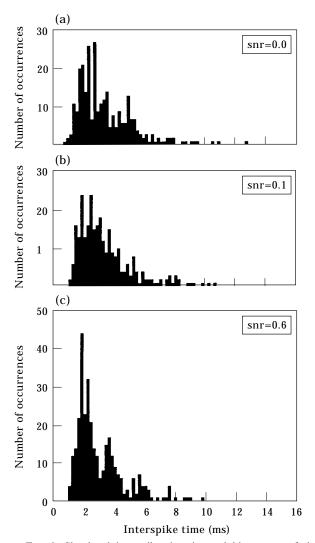
FIG. 8. Simulated interspike time interval histograms of the spiking activities in a single auditory nerve fiber for different signal-to-noise ratios (snr). (a) Spontaneous activity caused by the Brownian motion alone. The distribution is Poisson-like since the signal-to-noise ratio is 0, and is shifted by the smallest interspike time 0.8 ms—which is equal to the absolute refractory period of auditory nerve fibers. Increase of the signal-to-noise ratio results in the tendency that the histogram maxima coincide with multiples of the 2 ms period of the 500 Hz signal. The periodicity information is weakly represented in (b) where snr = 0.1, and can clearly be seen in the snr = 0.6 case (c). Simulation with the linear chain as a model for the stereocilia bundle with $\lambda = 0.2$ results in a noise amplitude of 2.2 nm r.m.s. Signal data: frequency 500 Hz, duration 3 s, amplitude 0, 0.22 and 1.32 nm; binwidth 0.2 ms.

This gradual effect is obvious from the interspike time histograms shown in Fig. 8 for signal-to-noise ratios of 0 (no signal at all), 0.1 (weak signal) and 0.6 (stronger signal, but still less amplitude than the noise), respectively.

We have analysed the information that is included in the time structure of simulated firing patterns of auditory nerve fibers that are stimulated with pure sinusoidal signals of low intensity. In this study the influence of the Brownian motion and the modification caused by the transformation of the mechanical to the electrical signal was substituted by low-pass filtering a combined 500 Hz sinusoidal and white noise signal. This signal was used as input to produce a firing pattern in the way as described in Fig. 7 in order to generate a series of interspike times. After being trained with a set of such firing patterns, a neural net was used to classify new auditory nerve patterns. From the time structure in a single fiber it needs about 2 s (= 200 interspike times in a fiber with a spontaneous rate of 100 spikes/s) to detect a signal that has an amplitude which is 10 times smaller than that of the noise. This result is equivalent to 20 ms signal duration, if one considers the spikes of 100 fibers coming from the same tonotopic region of the cochlea. Details of these investigations are reported in Gebeshuber et al. (1998b) and Rattay et al. (1998b).

The voltage fluctuations due to the Brownian motion are calculated for a standard IHC. A recent modeling study shows that this standard IHC is most sensitive for stimulation with 2 kHz (Gebeshuber et al., 1998a). Experimental investigations of the differences in the patterns of Brownian motion in IHCs from different locations along the cochlea are in preparation.

Discussion

An important result of our model of the Brownian motion of inner hair cell stereocilia is the root-mean-square displacement of 2 nm. A value of 3.5 nm was measured for the stereociliary bundle in the bull frog sacculus hair cell (Denk et al., 1989). An estimation of the root-mean-square amplitude can be made via the equipartition theorem and leads for the measured hair bundle stiffnes of 10^{-3} N/m (Howard & Ashmore, 1986) to a root-mean-square displacement of 2 nm (Hudspeth, 1989). The 2 nm r.m.s. value for the IHC stereociliary displacements is indeed a consequence of our model. In his approximation of the amphibian hair bundle r.m.s. displacement with the equipartition theorem, Hudspeth used the stiffness of the whole bundle. We use the stiffness of single mammalian stereocilia which yields a r.m.s. displacement of a single stereocilium of about 4.4 nm. Because of the connections between the stereocilia and their pre-tension the modeled r.m.s. displacement results in 2 nm.

The parameters that describe the mechanical properties of the stereociliary bundle vary because of experimental difficulties. Therefore it is necessary to

investigate the influence of parameter variations on the model of the Brownian motion of the stereociliary bundle. According to the equipartition theorem a smaller stiffness of the stereocilia would result in a larger mean displacement; however since the mean displacement is proportional to the square root of the spring constant, relatively large parameter variations result in rather small changes in the mean displacements. Decrease of the stiffness of the single stereocilia and constant coupling strength result in stronger correlation on the movements, since the relative influence of the elastic coupling of the stereocilia of the movement of the chain is reduced. Change in the damping constant β does not influence the mean displacement at all, but for the correlation of the displacements it is important that all inner degrees of freedom are overcritically damped, as assumed in our model. On the other hand a drastically reduced damping constant causes resonances in the system and a change in the correlation along the chain.

We have shown that besides the Brownian motion the stochastic components of transduction channel kinetics are responsible for the receptor potential changes and thereby for the spontaneous firing in the auditory nerve fibers. Other stochastic components which influence the spiking pattern are the variation in neurotransmitter availability and the distribution to the release zones, but investigations on the influence of these components are out of the scope of this model.

The main result of this investigation is that the threshold of auditory perception is not limited by the Brownian motion but in fact the noise supports the detection of weak signals by the mechanisms of stochastic resonance.

REFERENCES

BIALEK, W. & SCHWEITZER, A. (1987). Quantum noise and the threshold of hearing. *Phys. Rev. Lett.* **54**(7), 725–728.

DENK, W., WEBB, W. W. & HUDSPETH, A. J. (1989). Mechanical properties of sensory hair bundles are reflected in their Brownian motion measured with a laser differential interferometer. *Proc. Natl Acad. Sci. U.S.A.* **16**, 5371–5375.

FLOCK, A., FLOCK, B. & MURRAY, E. (1977). Studies on the sensory hairs of receptor cells in the inner ear. *Acta Otolaryngol.* **83**, 85–91.

GEESHUBER, I. C., PONTES PINTO, J., NAVES LEAO, R., MLADENKA, A. & RATTAY, F. (1998a). Stochastic resonance in the inner ear: the effects of endogenious transduction channel noise and stereociliary thermal motions on the human hearing threshold in various frequency bands. In: *Proc. TU-BioMed Symp.* 1998 '*Brain Modelling*' (Rattay, F., ed.) Vienna, ARGESIM Report 10, 40–44.

GEBESHUBER, I. C., MLADENKA, A., RATTAY, F. & SVRCEK-SEILER, W. A. (1998b). Brownian motion and the ability to detect weak auditory signals. In: *Chaos and Noise in Biology and Medicine* (Taddei-Ferretti, C., ed.) Singapore: World Scientific.

HARRIS, G. G. (1967). Brownian motion in the cochlear partition. *JASA* **44**, 176–186.

HOWARD, J. & ASHMORE, J. F. (1986). Stiffness of sensory hair bundles in the sacculus of the frog. *Hear. Res.* **23**, 93–104.

HUDSPETH, A. J. (1989). How the ear's works work. *Nature* **341**, 397–404.

PICKLES, J. O., COMIS, S. D. & OSBORNE, M. P. (1984). Cross-links between the stereocilia in the guinea pig organ of Corti, and their possible relation to sensory transduction. *Hear. Res.* **15**, 103–112.

RATTAY, F., GEBESHUBER, I. C. & GITTER, A. H. (1998a). The mammalian auditory hair cell: a simple electric circuit model. *J. Acoust. Soc. Am.* **103**, 1558–1565.

RATTAY, F., MLADENKA, A. & PONTES PINTO, J. (1998b). Classifying auditory nerve patterns with neural nets: a modeling study with low level signals. *Simulation Practice & Theory* **6**, 493–503.

RELKIN, E. M. & DOUCET, J. R. (1991). Recovery from prior stimulation. I—Relationsip to spontaneous firing rates of primary auditory neurons. *Hear. Res.* **55**, 215–222.

STEELE, C. R. & JEN, D. H. (1988). Mechanical analysis of hair cell microstructure and motility. In: *Cochlear Mechanisms* (Wilson, J. P. & Kemp, D. T., eds). New York: Plenum Press.

DE VRIES, H. L. (1948). Brownian movement and hearing. *Physica* **14**, 48–60.

ZETES, D. E. (1995). Mechanical and morphological study of the stereocilia bundle in the mammalian auditory system. Ph.D. Thesis, Stanford University.